Biogeochemistry (2025) 168:21
https://doi.org/10.1007/s10533-025-01213-y

Distinct impact of land use and soil development processes on coupled biogeochemical cycling of C, N and P in a temperate hillslope-flood plain system

Kaiyu Lei · Franziska B. Bucka · Christopher Just · Sigrid van Grinsven · Sebastian Floßmann · Michael Dannenmann · Jörg Völkel · Ingrid Kögel-Knabner

Received: 11 August 2024 / Accepted: 31 January 2025

Abstract Understanding the biogeochemical cycling of phosphorus (P), particularly organic P (OP) in soils, under varying land use and soil development processes is essential for optimizing P usage under P fertilizer crisis. However, the complexity of OP impedes the mechanistic understanding. Therefore, by using well-documented organic carbon (OC) and total nitrogen (TN) cycling, we studied their stoichiometric correlation with P in soil fractions to indicate soil organic matter (SOM) and P turnover under two land uses (Cropland VS. Grassland) in Germany. Our results showed that grassland soils on the hillslope have higher OC and TN stocks than cropland soils. Total P (TP) stocks were unaffected by land use. However, grassland topsoil exhibited higher OP stocks and OP/TP proportions than cropland, with a constant IP stock throughout the soil profile, as this was determined by soil development processes in the subsoil. This proves that the flood plain soils are decoupled from hillslope soils due to different soil development processes. The stoichiometric assessment revealed a higher enrichment of OP in fine fractions of grassland soils, indicating stronger resistance to P loss by soil degradation. Mechanistic insights from OC:OP ratio of fine fractions indicate two potential OP cycling pathways: a ratio similar to microbial biomass C:P ratio suggesting a greater OP stabilization within microbial biomass/necromass; whereas a narrower ratio indicating more OP associated directly with mineral surfaces. This study illuminates the complex interplay between land use and

Responsible Editor: Marie-Anne de Graaff.

Supplementary Information The online version contains supplementary material available at https://doi.org/10.1007/s10533-025-01213-y.

K. Lei (✉) · F. B. Bucka · C. Just · I. Kögel-Knabner
Chair of Soil Science, Technical University of Munich, Emil-Ramann-Straße 2, 85354 Freising, Germany
e-mail: kaiyu.lei@tum.de

F. B. Bucka
Soil Geography and Ecosystem Research, Goethe University Frankfurt, Altenhöferallee 1, 60438 Frankfurt am Main, Germany

S. van Grinsven · J. Völkel
Chair of Geomorphology and Soil Science, Technical University of Munich, Hans-Carl-von-Carlowitz-Platz 2, 85354 Freising, Germany

S. Floßmann · M. Dannenmann
Institute of Meteorology and Climate Research, Atmospheric Environmental Research (IMK-IFU), Karlsruhe Institute of Technology, Kreuzeckbahnstraße 19, 82467 Garmisch-Partenkirchen, Germany

I. Kögel-Knabner
Institute for Advanced Study, Technical University of Munich, Lichtenbergstraße 2a, 85748 Garching, Germany

Published online: 09 February 2025

soil development processes on OC, TN and P cycling, emphasizing the potential of stoichiometric assessment in soil fractions to understand OP biogeochemical cycling.

Keywords Land use · Soil organic matter · Phosphorus · Stoichiometry · Physical fractionation

Introduction

Continued high consumption of finite phosphate rock resources globally to produce phosphorus (P) fertilizers, driven by the increasing food demand, has sparked an intense debate on potential looming P scarcity or price spikes (Cordell and White 2011; Mew et al. 2023; Scholz et al. 2025). Concurrently, soil total P (TP) stocks loss (Hedley et al. 1982; Kopittke et al. 2017; Alt et al. 2011; Stutter et al. 2015) and soil degradation (Borrelli et al. 2017) have been exacerbated by natural vegetation land use changes toward cropland to meet growing food demands, further contributing to unsustainable P cycling. In response, a sustainable organic P (OP) management strategy has been recently proposed (Sulieman and Mühling 2021). To realize sustainable P use, there is a need for better understanding of P turnover under different land uses in the context of organic carbon (OC) and total nitrogen (TN) cycling.

The impact of land use and soil development processes on OC and TN stocks varies, especially between topsoil and subsoil. Topsoil OC stocks are strongly influenced by land use, with cropland use accelerating soil organic matter (SOM) mineralization, resulting in lower OC and TN stocks relative to grassland soils (Andreetta et al. 2023; Kögel-Knabner and Amelung 2021; Mayer et al. 2019; Wiesmeier et al. 2019; Gava et al. 2022). Conversely, soil development processes such as alluvial, colluvial, and pedogenic processes may lead to higher OC stocks in subsoils (Andreetta et al. 2023; Mayer et al. 2019).

In contrast to OC and TN stocks, TP stocks are predominantly determined by parent material rather than SOM input in mineral soils. Inorganic P (IP) comprises between 30 and 70% of TP stocks, with significant contributions from subsoils (25–70%) where IP dominates (Gocke et al. 2021; Kautz et al. 2013). The transition from natural vegetation to cropland alters the partitioning of IP and OP, though IP remains the dominant form (Hedley et al. 1982; Kopittke et al. 2017; Alt et al. 2011; Stutter et al. 2015). The partitioning of OP and IP is crucial for maintaining TP stocks against erosion-induced soil degradation due to their distinct stabilities.

Inorganic phosphorus is primarily stabilized as orthophosphate through occlusion, adsorption to surfaces (e.g., Al/Fe oxides, phyllosilicate edges, and SOM), precipitation with polyvalent cations and ligand exchange (Celi and Barberis 2005), in which the occlusion is the stabilizing processes of IP in the mineral matrix and aggregates involving a series of adsorption and precipitation processes. Conversely, organic phosphorus is stabilized mainly by sorption to charged mineral surfaces. Recent studies suggest that microorganisms can also stabilize and accumulate significant amount of OP, with a lower C:N ratio favoring higher OP stability (Sun et al. 2022). The stability of P is strongly correlated with the number of phosphate groups, with compounds like *myo*-inositol hexakisphosphate (IHP) showing greater stability compared to IP or other OP compounds with fewer phosphate groups (Gerke 2015). Studies have consistently shown that IP associated with clay minerals has a higher desorption rate and is less resistant to soil degradation than more stable OP compounds such as IHP (Sulieman and Mühling 2021). This instability may be further exacerbated by the lower affinity of IP for soil minerals compared to OP (Amadou et al. 2022).

Stabilization of P is especially critical on hillslopes, where soil loss is pronounced due to factors such as land use, slope steepness, precipitation, and surface roughness (Nguyen et al. 2016; Berhe et al. 2018). Particle size plays a crucial role, with smaller particles often exhibiting greater SOM resistance to erosion (Nguyen et al. 2016; Berhe et al. 2018), though recent studies also show that smaller particles can be eroded when forming macro-aggregates (Szabó et al. 2023). Compared to OC, some evidence suggest that most P is transported in particulate form, especially as particulate organic matter (POM) for OP, with agricultural land use being a significant contributor (Quinton et al. 2010). The extent of P transport is influenced by vegetation cover and supplemental P fertilizers (Berhe et al. 2018; Quinton et al. 2010). Quinton et al. (2010) emphasized a close relationship between soil resistance to erosion and SOM, with higher SOM leading to greater erosion

resistance. This raises questions about the stability of OP in smaller particles (Spohn 2020b) when associated with OC.

Despite these insights, few studies have investigated the partitioning of OP and IP across different soil particle sizes (Agbenin and Tiessen 1995; Spohn 2020b), with existing research indicating a higher accumulation of OP in clay-sized fractions. More work is needed to unravel how these dynamics influence P stability and erosion resistance under varying land use and soil development processes.

The cycling of OC, TN and P are strongly interrelated (Quinton et al. 2010). Well-established methods for studying OC and TN cycling, such as soil fractionation and stoichiometric analyses, may provide valuable insights for understanding P stabilization and cycling (Catoni et al. 2016; Guggenberger et al. 1994). Organic carbon has a longer turnover time in mineral-associated organic matter (MAOM) compared to POM due to strong organo-mineral complexes and physical protection from microorganisms (Schmidt et al. 2011). The stabilized OC in the MAOM fraction derives from both plant and microbial sources, with microbial biomass accounting for approximately 50% of OC (Angst et al. 2021; Kögel-Knabner 2002). These sources have significantly different OC:TN ratios: microbial biomass C:N ratio averages 9:1 (Cleveland and Liptzin 2007), while plant-derived biomass C:N ratios can reach to around 100:1 (Cotrufo et al. 2019; Kirkby et al. 2011; Tipping et al. 2016). The grassland in general has higher microbial biomass C:N ratio compared to cropland (Li et al. 2024). Despite these distinct C:N ratios in plant and microbial sources, the MAOM fraction maintains a relatively constant OC:TN ratio of approximately 12:1 in mineral soils. This narrow ratio is generally found in soils with OC assimilated into microbial biomass/necromass, bonded with minerals, and physically protected within aggregates (Kögel-Knabner 2008). Thus, the OC:TN ratio in the MAOM fraction can serve as a qualitative indicator for OC storage potential (Cotrufo et al. 2019; Kirkby et al. 2011).

Organic phosphorus is suspected to undergo comparable stabilization processes through assimilation within microbial biomass and subsequent association with mineral surfaces (Spohn 2020b). The MAOM fraction thus also maintains a relatively constant OC:P ratio around 200, especially OC:OP (Kirkby et al. 2011), compared to the ratios in the POM fraction, which varying from 100 to 6000 (Spohn 2020b). This observation has sparked interest in using stoichiometric correlations as an indicator for understanding OP stabilization and storage processes (George et al. 2018), considering a high variation of OC:OP ratios across different soil components: plant materials can approach 6000:1 (Cleveland and Liptzin 2007; Fanin et al. 2013), microbial biomass ranges from 23:1 to 100:1 in grassland and arable soils (averaging 60:1) (Cleveland and Liptzin 2007; Xu et al. 2013; Fanin et al. 2013; Griffiths et al. 2012; Heuck et al. 2015; Khan and Joergensen 2019; Turner et al. 2013; Wu et al. 2000), and mono/diester orthophosphate ranges from 1:1 to 11:1 (Condron et al. 2005). Although Kirkby et al. (2011) and Spohn (2020b) noted a relatively constant OC:OP ratio in the MAOM fraction, Williams and Steinbergs (1958) suggested that OP can also be associated with OC independently from N, derived from the findings of a weaker correlation of OP:TN compared to OC:TN ratios. Nevertheless, these uncertainties of the biogeochemical cycling of OP hinders its mechanistic understanding.

Given the critical role of OP in sustainable P utilization and its resilience against soil degradation (Sulieman and Mühling 2021), a deeper mechanistic understanding of OP interactions with SOM, soil microorganisms, and active mineral surfaces is required (George et al. 2018). To address these knowledge gaps and contribute to our understanding of biogeochemical processes controlling OC, TN and OP cycling in temperate ecosystems, we examine a temperate hillslope-flood plain system to answer the following questions:

- How do soil development processes and land use interact to determine the stocks of OC, TN, and P in topsoil and subsoil?
- What are the drivers underlying TP partitioning (IP vs. OP) and stoichiometric correlations of OC:TN and OC:OP across different soil fractions (POM vs. MAOM)?
- What are the implications of these stoichiometric correlations in soil different fractions for understanding OP stabilization mechanisms and cycling under different land uses and soil development processes?

To address these questions, we analyze bulk soils for OC, TN, TP, IP, and OP contents and stocks in a loess-affected hillslope-flood plain system under cropland and grassland use. The ^{15}N signature and ^{13}C solid-state nuclear magnetic resonance (NMR) spectroscopy give detailed information on the source of SOM and the retention of SOM. The further physical fractionation and stoichiometric analysis in fine (< 20 µm) and coarse (> 20 µm) soil fractions reflect the distribution and enrichment of SOM in these fractions, which are necessary for revealing their stoichiometric correlation and stabilization status, to recognize and differentiate pathways of OP cycling in the MAOM fraction.

To differentiate land use and soil development factors, we take advantage of investigating a periglacial loess loam-affected slope-flood plain system in a granitic region of the Bavarian Forest with documented historical land use and geomorphological information, which is a representative of slope-flood plain system in the low mountain range of the temperate zone.

Material and methods

Study site description

The study site is located near Süssenbach (49°06′12″ N, 12°21′37″ E) in the Falkensteiner Vorwald region, part of the Bavarian Forest in South-East Germany. The area has an annual mean temperature of 8.9 °C and an annual mean precipitation of 875 mm. The parent material is saprolite developed from granite (Regensburger Kristallgranit I) (Digitale Geologische Karte 1:25,000, 2022), which is also influenced by

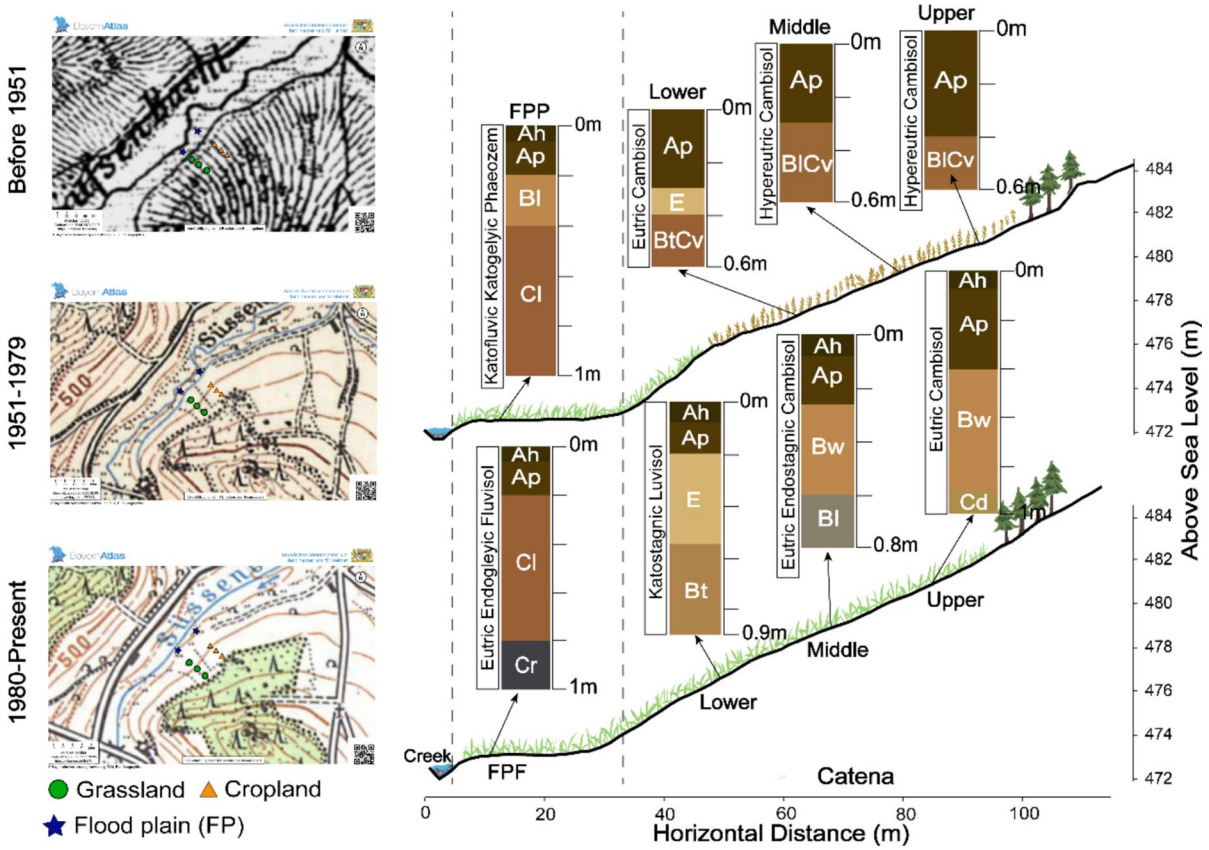

Fig. 1 Historic maps (BayernAtlas, Bayerisches Staatsministerium der Finanzen und für Heimat, 2023) and schematic graph of the study site Süssenbach. 'Upper', 'Middle', 'Lower', 'FPF', and 'FPP' means the upper, middle, and lower parts of the slope, Fluvisol, and Phaeozem in the flood plain, respectively. The soil properties are given in Tables S.1 and S.2

loess and slope deposits during the Late Pleistocene (Völkel 1995).

The study site includes an NNW-facing slope and a flood plain associated with the Otterbach creek (referred to as Süssenbach in historical maps, see Fig. 1). For clarity, the hillslope has been divided into upper, middle, and lower parts, which do not describe geomorphological features in the sense of a slope profile. The steepness of the slope is shown in Table S.1. Historical maps indicate that deforestation occurred in 1950, converting the slope into cropland and grassland (grassland was temporarily used as cropland evidenced by the existence of an Ap horizon, Fig. 1). The flood plain was a natural grassland without active management since at least 1890 but has been under regular grassland management since 1980, as depicted in historical maps (Fig. 1). The Otterbach, a second-order tributary of the Danube confluence at Sulzbach (Opf.), runs at an elevation of 473 m above sea level in this region. The Otterbach was meandering and received limited management until it was straightened in 1980. The annual mean discharge of Otterbach from 1957 to 2013 is 0.833 $m^3\ s^{-1}$ (0.156 $m^3\ s^{-1}$ annual minimum discharge and 11 $m^3\ s^{-1}$ annual maximum discharge) according to Bayerisches Landesamt für Umwelt (2023).

According to the World Reference Base for Soil Resources (WRB 2015), the soil types in the study area are classified as Cambisols on the hillslope, except the lower part of the grassland, which is classified as Luvisol. A Fluvisol (FPF) and a Phaeozem (FPP) were found in the flood plain (Fig. 1). A detailed soil description is provided in the Supplementary Material.

Since 1995, the cropland has been under intensive organic management. It was previously treated with Carbonic Magnesium for liming purposes. Annually, the cropland receives cattle slurry fertilization at a rate of 15 $m^3\ ha^{-1}$ in both spring and autumn. Since 1995, the grassland has been under extensive management, receiving the same type and amount of fertilizer as cropland: two slurry applications per year of 15 $m^3\ ha^{-1}$ each. In a few years, the second grassland fertilization was conducted with farmyard manure instead of slurry, but overall, the fertilization is very similar between grassland and cropland. The flood plain has been managed similarly to the grassland on the slope since 1995. However, a 10 m zone beside the Otterbach has yet to be fertilized in compliance with the Fertilization Regulation issued according to the Water Framework Directive (2000/60/EG). The composition of floristic species is detailed in the Supplementary Material.

Soil sampling and pretreatment

For both types of land uses on the slope, soil profiles were opened in the upper, middle, and lower parts of the slope. In the flood plain, two soil profiles were opened approximately 7 m from the Otterbach. Soil samples for bulk density analysis were collected in triplicates for each horizon using stainless steel cylinders (100 cm^3). Additionally, three undisturbed soil cores 2–3 m in proximity to each soil profile were drilled using motor driller (Cobra TTe, Atlas Copco, Germany) to a depth of 1 m, used as three replicates of the corresponding soil profile at an increment of 20 cm, which were used for further stock calculation with the soil samples collected from the open soil profile. All fresh samples were stored at 4 °C prior to air-drying at 20 °C. The topsoils (0–20 cm) obtained from soil profile and drilling cores, they were further separated at fixed depths 0–5 cm, 5–10 cm, and 10–20 cm for bulk soil $\delta^{15}N$ natural abundance isotopic signature. These samples were oven-dried at 55 °C.

Fresh soil samples collected for bulk density estimation were oven-dried at 105 °C for 24 h, after which the total bulk density of the soil samples was calculated. The dried soils were carefully sieved to remove rock fragments (≥ 2 mm). Visible root remnants were identified and removed. The calculation of bulk density without rock fragments (BD_{fine}) was simplified using the following Eq. (1):

$$BD_{fine} = \frac{Dry\,Mass_{total} - Dry\,Mass_{rock\,fragments}}{Volume_{total} - \frac{Dry\,Mass_{rock\,fragments}}{\rho_{rock\,fragments}}} \quad (1)$$

where BD_{fine} (g cm^{-3}) is the bulk density without rock fragments, Dry $Mass_{total}$ (g) is the total mass of the dried sample, and Dry $Mass_{rock\ fragments}$ is the mass of rock fragments. $Volume_{total}$ (cm^3) is the total volume of the sample, equivalent to the volume of the stainless-steel cylinder. The density of rock fragments ($\rho_{rock\ fragments}$) is approximately 2.6 g cm^{-3}.

The collected soil samples were air-dried at 20 °C and sieved through a 2 mm mesh, excluding any visible root remnants, to ensure consistent particle size for physical fractionation, texture, pH, and P analysis. A portion of the sieved samples, thoroughly mixed, were ball-milled at a frequency of 25 Hz for 2 min to facilitate subsequent OC, TN, TP and $\delta^{15}N$ analysis.

Physical and chemical analysis

Soil texture and pH analysis

For soil texture analysis, soils with an OC content higher than 15 mg g^{-1} were dispersed with 0.025 M $Na_4P_2O_7$ before organic matter removal with 30% H_2O_2. Approximately 20 g of dry soil was then moistened with 25 ml 0.1 M $Na_4P_2O_7$, followed by the addition of 200 ml of water. The mixture was dispersed in an ultrasonic bath for 10 min and shaken overnight. The soil was separated into sand (2000–63 µm), silt (63–2 µm), and clay (< 2 µm) particles using the Koehn pipette and sieves (Kretzschmar 1996).

The pH in the soil solution was analyzed using the 0.01 M $CaCl_2$ extraction method, with a soil-to-extractant ratio of 1:2.5 (w/v). The extracts were analyzed by a pH meter (Seven Easy pH, Mettler-Toledo, Switzerland).

Carbon, nitrogen and phosphorus content and stock analysis, $\delta^{15}N$ signature

Total C and TN were determined using a dry combustion method at 1000 °C, with the EuroEA Elemental Analyser (HEKAtech, Wegberg, Germany). Samples with pH (0.01 M $CaCl_2$) greater than 6 were tested using a Scheibler Calcimeter for inorganic C. As the detected inorganic C was less than 2%, total C was subsequently used to refer to OC in further analysis.

TP, as well as other total elements including sodium (Na), calcium (Ca), magnesium (Mg), and aluminum (Al) were determined by a mixture of concentrated $HClO_4$–HNO_3–HF–HCl method (Page et al. 1982). The ball-milled bulk soils were digested stepwise with $HClO_4$-HNO_3 mixed solution (1:1 v/v), HF, and $HClO_4$ to break down and oxidize SOM and dissolve silicates. The digested residues were further treated with HCl and heated overnight at 60 °C to solubilize inorganic matter. The solution was analyzed by inductively coupled plasma-optical emission spectrometry (ICP-OES, Varian Vista-Pro CCD).

A modified sulfuric acid method was employed to determine OP (Saunders and Williams 1955; Walker and Adams 1958). OP content was calculated as the difference of orthophosphate determined from pre-muffle furnace ignited soil (550 °C, 1 h) and non-ignited soil after extracted with 0.5 M H_2SO_4 for 16 h. Extracts were filtered through Munktell 131 filter paper (< 5 µm) (Ahlstrom Munksjo) for further analysis by ICP-OES. IP was then determined by subtracting OP from TP.

The stocks of OC, TN, TP, OP, and IP were estimated using Eq. (2) (Hobley et al. 2018):

$$X_{stocki} = X_{concfinesoil} \times BD_{fine} \times Depth_i \times (1 - rock\,fragments\,fraction) \quad (2)$$

where $X_{stock\,I}$ represents the stock of specific nutrients at a specific depth, $X_{conc\ fine\ soil}$ represents the nutrient content at a specific depth, and rock fragments fraction represents the mass fraction of rock fragments.

The $\delta^{15}N$ analysis of the bulk soils was conducted using a Costech elemental analyzer (Costech International S.p.A., Milan, Italy) coupled to a Thermo Finnigan Delta V Plus isotope ratio mass spectrometer (Thermo Scientific, Waltham, MA, USA). The detailed procedure was described by Liu et al. (2015).

^{13}C solid-state nuclear magnetic resonance (NMR) spectroscopy

The chemical compositions of bulk soil OC were analyzed using ^{13}C CP-MAS solid-state NMR (Bruker DSX 200, Bruker BioSpin GmbH, Karlsruhe, Germany). The ball-milled soils were filled into 7 mm zirconium dioxide rotors and spun in a magic angle spinning probe at a rotation speed of 6.8 kHz, with an acquisition time setting of 1 ms. The relative signal intensity of the chemical shift was recorded for quantification based on the four spectral regions assigned as: alkyl-C (10–45 ppm), O-alkyl-C (45–110 ppm), aryl-C (110–160 ppm), and carboxyl-C (160–220 ppm) (Mueller and Koegel-Knabner 2009). The decomposition state was referred to as the alkyl:O-alkyl-C ratio. The

molecular mixing model revised by Nelson and Baldock (2005) was applied to infer molecular structures following chemical shift regions: 0–45, 45–60, 60–95, 95–110, 100–145, 145–165, and 165–215 ppm, estimating six components including carbohydrate, protein, lignin, lipid, carbonyl, and char. The char content based on this approach was the minimum amount (Paetsch et al. 2017).

Physical fractionation

A simple particle size fractionation method was applied to fractionate bulk soil into a fine fraction (< 20 µm) and a coarse fraction (20–2000 µm) with distinct SOM turnover times (Just et al. 2021). In short, approximately 10 g of air-dried soil (2 mm sieved) was re-wetted and dispersed using ultrasonication with a total energy input of 450 J ml^{-1}. The dispersed sample was carefully sieved through 20 µm mesh with 2 l purified H_2O by hand using a rubber spatula. The suspension that passed through was defined as the fine fraction, containing mainly the MAOM fractions. The remaining materials were transferred to another container with purified H_2O and further cleaned in an ultrasonic bath for 5 min, regarded as the coarse fraction, containing mainly the POM fractions. The MAOM fraction contains MAOM and fine particle-size classes (clay-middle silt < 20 µm) and the POM fraction contains POM and coarse particle-size classes (coarse silt-coarse sand > 20 µm). Both fractions were dried in the oven at 60 °C and subjected to the same analysis procedure for OC, TN, and P as the bulk soil.

Statistical analysis

Stock differences between land use on the slope, and between the slope (cropland + grassland) and flood plain were investigated to compare the effects of land use and soil development processes. The A horizon within soil profiles on the slope and the flood plain was compared with respect to NMR relative proportion of chemical shift regions of OC and stoichiometric correlation between OC, TN, and OP.

Due to the lack of land use replicates within the slope, linear mixed effects models were employed to enhance statistical inference with non-independent replicates. Random effects that could contribute to stock differences due to site variations, such as slope parts and soil types, were considered. The variance between pseudo-replicates within specific slope parts was also included as a random effect. Fixed effects, including depth, land use, and weathering index, were used to investigate how these factors influenced the nutrient content at different depths and to identify the dominant factor regulating OC, TN, TP, OP, and IP contents. Variance inflation factors (VIF) were used to avoid multicollinear predictors, excluding those predictors with VIF > 5. Only land use was set as a fixed effect for stocks in 0–20 and 0–60 cm. Marginal and conditional pseudo-coefficients (R^2_m and R^2_c) were calculated to explain the variance by fixed effects and by both fixed effects and random effects (Nakagawa and Schielzeth 2013). Detailed statistical information is provided in Table S.3.

If the linear mixed effects model indicated a significant effect of land use, a two-way ANOVA was applied to compare the two land uses on the slope and to compare the slope and flood plain (Table S.4). The Levene Test and Shapiro Test were used to validate the dataset homogeneity and test the normality of residuals. The TukeyHSD test was applied for post-hoc analysis. Natural logarithmic transformation was used for skewed datasets not meeting normality assumptions. Linear and logarithmic regression models were used to investigate the stoichiometric correlation in the bulk, fine, and coarse fractions in the A horizon.

The statistical analyses were conducted in software R (V4.3.1; R Core Team 2023), with packages including 'readxl' (V1.4.3; Wickham and Bryan 2023), 'lme4' (Douglas et al. 2015), 'Matrix' (V1.6.3; Bates et al. 2023), 'lmerTest' (Kuznetsova et al. 2017), 'car' (Fox and Weisberg 2019), 'margins' (V0.3.26; Thomas et al. 2021), 'ggplot2' (Hadley 2016), 'ggpubr' (V0.6.0; Kassambara 2023), 'RColorBrewer' (V1.1.3; Neuwirth 2022) and 'ggsignif' (Ahlmann-Eltze and Patil 2021).

Results

Description of soil profiles in the study site

In the cropland, the soil types from the upper part to the lower part of the hillslope are Hypereutric Cambisols, Hypereutric Cambisols, and Eutric Cambisol. In the grassland, they are Eutric Cambisol, Eutric

Endostagnic Cambisol, and Katostagnic Luvisol. To assess soil development status from the parent material, we employed the Chemical Index of Weathering (CIW) (Harnois 1988). This index, the ratio of Al to (Al + Ca + Na), has been claimed to adequately predict the weathering status in semi-humid and humid climate conditions (Heidari et al. 2022). The CIW on the slope ranged from 75 to 86 in the grassland and 77 to 85 in the cropland. ANOVA results (Table S.5) showed no significant differences in CIW values between the two land uses on the slope, suggesting uniform geochemical weathering conditions on the hillslope.

The flood plain soil below the slope under cropland use is classified as Katofluvic Katogelyic Phaeozem. Conversely, the flood plain beneath the slope under grassland use is classified as Eutric Endogieyic Fluvisol (Fig. 1). The basic properties of the soil profiles are given in Table S.1 and the detailed soil description is provided in the Supplementary Material.

Bulk soil OC, TN, TP, OP, IP contents, and $\delta^{15}N$ signature

The mean OC, TN, and OP contents in topsoil (0–20 cm) of the grassland on the slope were higher than the cropland. As shown in Table S.7, the OC, TN, and OP decreased with depth in grassland topsoil, from up to 65 mg OC g^{-1}, 4.7 mg TN g^{-1} and 0.79 mg OP g^{-1} to 13 mg OC g^{-1} and 1.3 mg TN g^{-1} and 0.43 mg OP g^{-1}, which was in contrast to the consistent content observed in cropland topsoil around 16 mg OC g^{-1} and 1.6 mg TN g^{-1} and 0.45 mg OP g^{-1}. However, a sharp decline in OC and TN content was observed in the BC horizon of the cropland soil below 40 cm.

The $\delta^{15}N$ values in cropland topsoil (0–20 cm) were unaffected by depth, ranging between 6 and 7 ‰ (Fig. S.2). In contrast, the grassland $\delta^{15}N$ values were significantly lower (3–4.5 ‰) in the 0–5 cm depth and increased with depth, matching cropland values at 10–20 cm. (Fig. S.2).

The OP distribution in bulk soil varied between land use. The grassland topsoil was enriched with OP, with an OP/TP proportion greater than 50%, averaging up to 67%. In contrast, the cropland topsoil was dominated by IP, with an OP/TP proportion consistently below 50%, dropping to 20% or lower in the subsoil (Table S.7). IP remained constant in the subsoil of the slope. Statistical analysis revealed significant differences in OC, TN, TP, and OP between land use on the slope (Table S.3).

No differences in OC and TN content were observed between the two soil types, FPF and FPP, in the flood plain for both topsoil and subsoil (Table S.7). A higher mean IP content was observed in FPF compared to FPP, with both TP content being dominated by IP.

Bulk soil OC, TN, TP, OP and IP stocks

The linear mixed model was utilized to investigate the impact of land use on OC, TN, and P stocks. This model extends the linear model to analyze non-independent datasets, addressing the potential site effect that may overshadow the land use effect without replicating sites (UCLA 2021). The model revealed that random effects accounted for up to 40% of the variance, attributed to factors other than fixed effects, derived from the difference between R^2_c and R^2_m (Table S.3). The influence of random effects varied with different elements and depths, showing no significant difference in TN, TP, and OP between land use in the topsoil (0–20 cm) and no significant difference in TP and IP when including the subsoil (20–60 cm). Only OC stocks were significantly affected by land use in both topsoil and subsoil (Table S.3).

In the topsoil (0–20 cm), grassland on the slope showed significantly higher OC stocks (40 Mg OC ha^{-1}) but significantly lower IP stock compared to cropland (30 Mg OC ha^{-1}) (Fig. 2; Tables S.3, S.4). Two-way ANOVA results highlighted significantly higher OC stock in the lower part of grassland compared to cropland (Table S.4).

Considering the increment from 20 to 60 cm, TN and OP were significantly higher in the grassland on the slope than in the cropland, while the significantly higher OC stock in the grassland remained present (Table S.2). The mean OC, TN, and OP in the grassland reached 71 Mg OC ha^{-1}, 6.5 Mg TN ha^{-1}, and 2.2 Mg OP ha^{-1}, respectively. In comparison, the cropland showed stocks of 50 Mg OC ha^{-1}, 4.7 Mg TN ha^{-1}, and 1.7 Mg OP ha^{-1} (Fig. 2). TukeyHSD results revealed significantly higher OC and TN stocks in the middle and lower parts of grassland on the slope compared to cropland (Table S.3). The OC and TN stocks in the 0–60 cm soil of both land uses on the slope were concentrated in topsoils (0–20 cm).

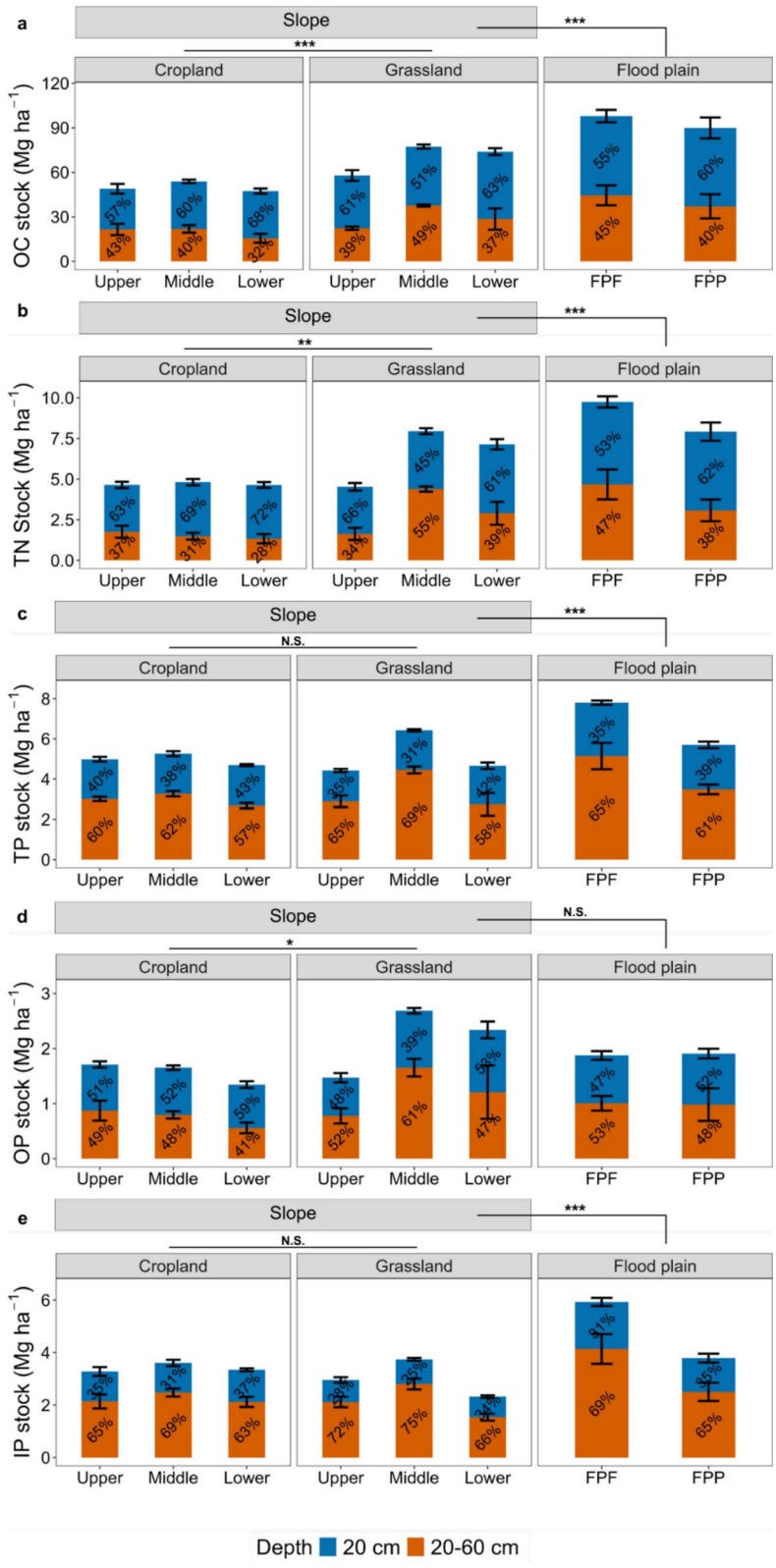

Fig. 2 The accumulated stock of **a** OC, **b** TN, **c** TP, **d** OP, and **e** IP in 0–20 cm (Orange) and 20–60 cm (Blue) depths between land uses on the slope, and between the slope and the flood plain. The data were derived from soil profile and three corresponding soil cores in proximity to it. The bulk density of the soil profile was used for the stock estimations. Data are mean ± SE, n = 4. The 'Upper', 'Middle', and 'Lower' mean the upper, middle, and lower parts of the slope. The FPF and FPP mean the Fluvisol and Phaeozem in the flood plain, respectively. The asterisk in 'Cropland' and 'Grassland' means the significant level of 0–60 cm stocks between land use on the slope, and the asterisk in 'Flood plain' means the significant level of 0–60 cm stocks between the slope and flood plain from ANOVA. The asterisk ('*') indicates $0.01 < p < 0.05$, '**' indicates $0.001 < p < 0.01$, '***' indicates $p < 0.001$. The non-significant comparison is marked as 'N.S.'. Detailed statistical results are shown in Table S.4

The topsoil (0–20 cm) was identified as the primary reservoir for IP stock in the cropland, with a consistent OP/TP proportion of 39–43%, regardless of variations in TP and OP stocks (Table S.6). In grassland, the OP stock proportion increased from 46% in the upper part to 58% in the lower part. Considering the subsoil (20–60 cm), IP stock predominated on the slope regardless of land use (Table S.6).

No significant differences in topsoil stocks were found between the slope and the flood plain (Table S.4; Fig. 2). However, the flood plain is significantly higher in OC, TN, TP, and IP stocks when including the subsoil. OP stock was similar between the slope and flood plain.

Molecular components of bulk soil derived from ^{13}C solid-state NMR spectroscopy

The A horizon of the soil profiles was analyzed using ^{13}C solid-state NMR spectroscopy. Except for the upper part of the slope, the grassland exhibited a higher proportion of O-alkyl-C and a narrower alkyl:O-alkyl-C ratio compared to the cropland at their corresponding parts (Table 1). In both land uses, the alkyl:O-alkyl-C ratio tended to decline from the upper to the lower part of the slope. Results from the molecular mixing model revealed that the soil in the A horizon of the grassland had a higher carbohydrate content, averaging up to 34%. However, a lower lignin content compared to the cropland (Table S.8). Across all soils, 3 to 6% of char was detected.

On the slope, a linear correlation was identified between the alkyl:O-alkyl-C ratio and the OC:OP ratio as well as between alkyl:O-alkyl-C ratio and OC:TN ratio in the fine fraction (Table S.9). In the flood plain, a linear correlation was found only between the alkyl:O-alkyl-C ratio and the OC:OP ratio (Table S.9). Higher OC:OP ratio and OC:TN ratio were associated with narrower alkyl:O-alkyl-C ratios (Table S.9).

The distribution and enrichment of OC, OP, and macronutrients in the fine and coarse fractions

Within the A horizons of the soil profiles (Fig. 3), both OC and OP were predominantly concentrated in the fine fraction for both land uses on the slope, ranging from 70 to 83% for OC and 84% to 93% for OP. The proportion of OP in the fine fraction was higher than that of OC. Additionally, the OC and OP content in both the fine and coarse fractions increased with the OC and OP content in bulk soil. Figure S.1 shows that the OP/TP proportion was higher on the slope than on the flood plain.

To compare the enrichment of OC, TN, OP, and total elements in the fine and coarse fractions relative to the bulk soil, an enrichment factordefined as the ratio of the content in the fraction to the content in bulk soil (mg g^{-1} the fraction/mg g^{-1} the whole soil, >1 means enrichment), was introduced to exclude the effects of different SOM levels in bulk soil (Christensen 1992; Guggenberger et al. 1994). The results showed enrichment factors above 1 for OC, TN, OP, Fe, and Mg in the fine fraction of all soils, regardless of land use. OP showed higher

Table 1 Integrals of the relative proportion of chemical shift regions of OC in the A horizon of the soil profile on the slope and in the flood plain. The FPF and FPP mean the Fluvisol and Phaeozem in the flood plain, respectively

Location	Part	Carboxyl-C	Aryl-C	O-Alkyl-C	Alkyl-C	Alkyl:O-Alkyl-C ratio
Grassland on the slope	Upper	15 ± 2	24 ± 3	42 ± 5	18 ± 1	0.44 ± 0.11
	Middle	14 ± 0	23 ± 3	47 ± 2	16 ± 1	0.35 ± 0.04
	Lower	14 ± 1	20 ± 2	48 ± 2	18 ± 1	0.37 ± 0.04
Cropland on the slope	Upper	16 ± 1	25 ± 0	40 ± 1	18 ± 0	0.45 ± 0.02
	Middle	15 ± 1	26 ± 0	42 ± 1	17 ± 0	0.45 ± 0.04
	Lower	15 ± 1	23 ± 0	43 ± 2	18 ± 1	0.41 ± 0.03
Flood plain	FPF	16 ± 1	21 ± 1	46 ± 4	18 ± 1	0.46 ± 0.11
	FPP	14 ± 1	22 ± 1	45 ± 4	17 ± 1	0.51 ± 0.14

Data are the mean value of each depth in the A horizon ± SE

enrichment in the fine fraction than OC and TN, with a higher enrichment factor in the fine fraction and a lower enrichment factor in the coarse fraction. Total Ca was enriched in the coarse fraction on the slope and in the fine fraction on the flood plain, while total Al was balanced between the two fractions.

In the fine fraction, OP dominated the TP pool in both land uses, with a significantly higher proportion of OP in soils under grassland than cropland on the slope (Table 2). Conversely, the TP pool was primarily composed of IP in the coarse fraction, with OP constituting less than 10% of the TP pool. No significant difference in the OP proportion in the coarse fraction was observed between land use.

On the slope, a linear regression model revealed strong correlations among OC and TN, OC and OP, and OP and TN in the fine fraction (Table S.10). However, the fine fraction in the flood plain showed no correlation between OP and either OC or TN, while a similar correlation between OC and TN, compared to the slope, was found (Table S.10). Detailed statistical results are presented in Table S.10.

OC:TN ratio to OC:OP ratio and their correlation with OC in bulk soils, fine and coarse soil fractions

The variation in the ratio of OC to OP with depth is shown in Fig. 4a. In the grassland on the slope, the OC:OP ratio exhibited a sharp decline in the uppermost 0–10 cm, followed by a relatively stable distribution with values of approximately 30:1 across depths. A similar trend was observed in the flood plain, albeit with a stabilized ratio at approximately 50:1. In contrast, the cropland maintained a consistent OC:OP ratio around 30:1 in the A horizon, decreasing to 10:1–20:1 in the B horizon. Overall, the flood plain displayed a higher OC:OP ratio compared to the slope, ranging from 42:1 to 80:1.

Distinct OC:TN and OC:OP ratios were observed between the fine and coarse fractions. In the fine fraction, the OC:TN ratio ranged from 9:1 to 13:1, while the OC:OP ratio ranged from 19:1 to 61:1. On the other hand, the coarse fraction exhibited a wider range of OC:OP ratios, spanning from 90:1 to 550:1 (Fig. 4).

In the cropland, there was no linear correlation between OC:TN ratio and OC:OP ratio for both bulk soil and the fine fraction (Fig. 4b, c), whereas a linear correlation was evident in the grassland on the slope. In contrast to the bulk soil and the fine fraction, the coarse fraction showed distinct relationships between the OC:TN ratio and OC:OP ratio. Specifically, a linear correlation was found in the cropland on the slope as well as in the flood plain, indicating that a higher OC:OP ratio was corresponded to a higher OC:TN ratio.

Logarithmic regression was performed on the natural log-transformed OC:TN ratio (Fig. 5c) and OC:OP ratio (Fig. 5d) in the bulk soil and fine fraction on the slope, and in the flood plain (Fig. 5a, b). No correlation was found in the coarse fraction. The results revealed an increasing trend of both the OC:TN and the OC:OP ratios with higher OC content. However, once the OC content reached approximately 85 mg OC g^{-1}, the OC:TN ratio remained below 12:1 and the OC:OP ratio remained below 90:1 in both land uses. No correlation was found between OC:TN ratio and OC content in either bulk soil or the fine fraction.

Across different land uses on the slope, the OC:TN and OC:OP ratios were consistently higher than 12:1 and 72:1, respectively. The relationship between OC content and the OC:TN ratio and OC:OP ratio suggested that higher OC content corresponds to elevated OC:TN and OC:OP ratios in both soil fractions (Fig. 5). The order of OC:TN ratio and OC:OP ratio was as follows: coarse fraction > bulk soil > fine fraction.

Discussion

Soil development effects overrule management effects on OC, TN, and P stocks in the flood plain (and vice versa on the hillslope)

Under similar soil development processes and similar organic fertilization regimes over 30 years on the hillslope, the grassland shows significantly higher OC stocks in both topsoil (0–20 cm) and subsoil (20–60 cm) compared to cropland (Fig. 2a, b). This difference stems from higher OC content in the topsoil (Table S.7) due to greater SOM input, faster root turnover (Fig. S.2), and a well-developed, preserved B horizon. In contrast, the cropland exhibits significantly lower stocks due to reduced SOM input from harvesting, evidenced by a higher alkyl:O-alkyl-C ratio (Table 1), soil structure degradation as shown

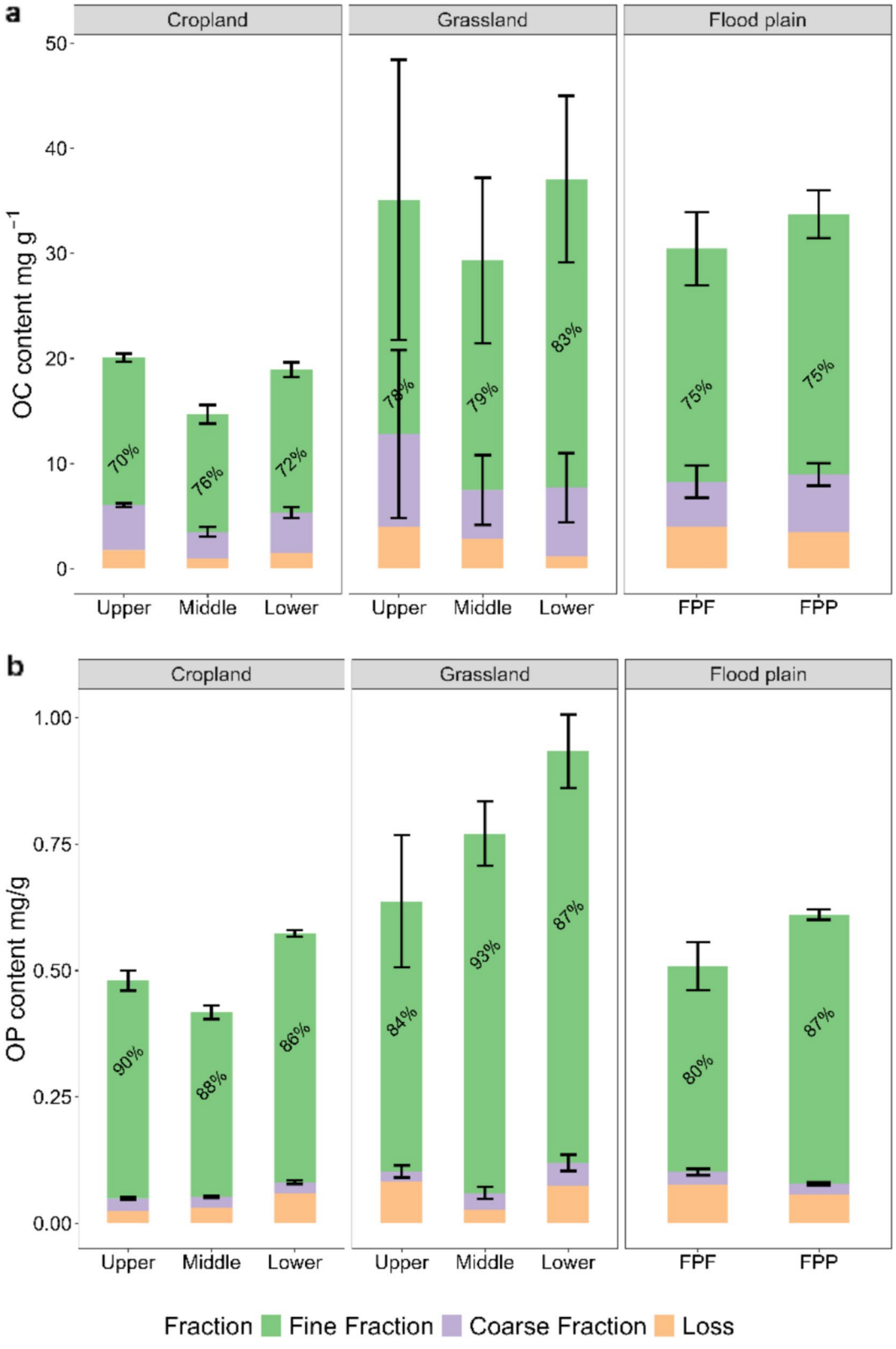
a
Cropland
Grassland
Flood plain
OC content mg g^{-1}
50
40
30
20
10
0
70%
76%
72%
78%
79%
83%
75%
75%
Upper
Middle
Lower
Upper
Middle
Lower
FPF
FPP
b
Cropland
Grassland
Flood plain
OP content mg/g
1.00
0.75
0.50
0.25
0.00
90%
88%
86%
84%
93%
87%
80%
87%
Upper
Middle
Lower
Upper
Middle
Lower
FPF
FPP
Fraction
Fine Fraction
Coarse Fraction
Loss

◂**Fig. 3** The **a** OC and **c** OP content in the A horizon of each soil profile depicted for cropland and grassland on the slope and **b** OC and **d** OP content depicted for the A horizon of each soil profile of slope and flood plain. Samples were collected at different depths in the A horizon. The FPF and FPP mean the Fluvisol and Phaeozem in the flood plain, respectively. Data are the mean value of each depth in the A horizon ± SE. The loss fractions were presented as the mean values only

by the OC:Clay ratio-derived index (Table S.2) (Prout et al. 2021), and soil loss, indicated by BC horizons following ploughed A horizons (Chaplot and Poesen 2012; Van Oost et al. 2007) and higher bulk density (Table S.1). TN stocks are only significantly higher in the subsoil of grasslands, while the topsoil shows no marked differences between land uses (Table S.3), which is consistent to a lower $\delta^{15}N$ signature (Fig. S.2), which indicates better N retention and lower gaseous N loss.

Due to the different origins of P, the impact of land use on P pools is not as straightforward as observed for OC and TN (Condron et al. 2005). While OP originates from SOM and biological processes, IP is primarily determined by parent material (Gocke et al. 2021). For the OP content, the enhanced SOM accumulation in grassland soils is connected to a higher OP content in the topsoil (Table S.7), and a well-preserved B horizon further results in significantly higher OP stocks throughout the soil profile. No significant difference was found in OP stocks of the cropland topsoil compared to the grassland topsoil, which is due to the higher bulk density compensating for the lower mean OP content (Table S.1). A similar weathering state of the parent material between the two land uses at our study site, as indicated by comparable CWI values (Table S.6), results in a relatively constant IP content with depth, irrespective of land use, and a higher bulk density in cropland further leads to significantly higher IP stocks, consistent with other cropland soils (Cade-Menun et al. 2017; Stutter et al. 2015; Von Sperber et al. 2017). As a result, this compensatory effect on IP stocks in cropland topsoil counterbalances the depletion of OP stocks in the subsoil, resulting in comparable TP stocks between the two land uses (Table S.3; Fig. 2). The TP stock at 0–60 cm depth in both land uses is IP-dominated (Table S.6), with subsoil contributing higher IP stocks regardless of land use.

In contrast, the flood plain under extensive grassland use reveals higher OC, TN, TP and IP stocks compared to hillslope soils throughout the profile (Fig. 2; Table S.4), primarily due to significant contributions from the subsoil. The subsoil in the flood plain is developed from alluvial sedimentation and influenced by groundwater, as evidenced by thick Cl/Cr horizons and documented historical maps (Fig. 1). This results in higher SOM accumulation through inundation and sedimentation in the subsoil (Martinez-Mena et al. 2019; Mayer et al. 2018), leading to significantly higher OC and TN stocks (Table S.4). Additionally, the subsoil in the flood plain has significantly higher IP stocks, possibly due to P sorption from groundwater (Weihrauch and Weber 2021), which contributes more to the TP stocks than the hillslope subsoil (Table S.6). No significant difference in OC, TN, and P was found in the topsoil (A horizon), which was primarily impacted by grassland use, as evidenced by the presence of the Ah horizon (Fig. 1).

The stocks of topsoil and subsoil disentangle the distinct impacts of land use and soil development processes on OC, TN, and P stocks, considering both topsoil and subsoil. Under similar soil development processes, grassland soils on the hillslope show higher OC and TN stocks due to greater SOM input and a well-preserved B horizon, while cropland soils show lower stocks from reduced SOM input and soil degradation. The responses of P pools differ, with OP being influenced by land use (SOM input) and IP primarily determined by soil development processes. The higher IP stocks in the cropland topsoil counterbalance the lower OP stocks in the subsoil, resulting in comparable IP-dominated TP stocks between land use. The flood plain, decoupled from the hillslope due to different soil development processes, shows significant OC, TN and IP stock contributions from the subsoil, with land use effects confined to the topsoil.

The cropland soils tend to be less resistant to soil P loss by degradation, as indicated by less enrichment of OP in the fine fraction

The OC, TN, and P stocks provide an overall map of their distribution and abundance in topsoil and subsoil, reflecting the impacts of land use and soil development processes. This distinct distribution prompts interest in factors controlling their availability and stabilization, especially P, which are also essential for long-term management regimes in the face of

Table 2 The OC:TN:OP stoichiometry in the fine and coarse fraction of the A horizon in soils. The enrichment factor is calculated by the OC/TN/OP content in each fraction divided by the OC/TN/OP content in bulk soil. The FPF and FPP mean the Fluvisol and Phaeozem in the flood plain, respectively

Location	Part	Fraction	OC:TN	OC:OP	OP/TP	OC Enrichment Factor	TN Enrichment Factor	OP Enrichment Factor	Al Enrichment Factor	Ca Enrichment Factor	Mg Enrichment Factor
					%						
Grassland on the slope	Upper	Fine	10 ± 1.0	35 ± 13	66 ± 8	1.9 ± 0.40	2.0 ± 0.39	2.0 ± 0.21	1.2 ± 0.06	0.80 ± 0.01	1.6 ± 0.12
		Coarse	32 ± 7.1	251 ± 151	4.5 ± 0.37	0.30 ± 0.17	0.17 ± 0.13	0.05 ± 0.03	0.85 ± 0.02	1.1 ± 0.05	0.43 ± 0.02
	Middle	Fine	11 ± 0.5	30 ± 8.4	75 ± 1.0	1.7 ± 0.22	1.8 ± 0.34	1.9 ± 0.07	1.1 ± 0.03	0.90 ± 0.05	1.6 ± 0.08
		Coarse	19 ± 2.6	120 ± 57	7.4 ± 2.7	0.28 ± 0.11	0.17 ± 0.05	0.08 ± 0.02	0.87 ± 0.01	1.2 ± 0.06	0.44 ± 0.02
	Lower	Fine	10 ± 0	35 ± 6.5	86 ± 2.0	1.7 ± 0.18	1.8 ± 0.18	1.8 ± 0.05	1.1 ± 0.03	0.99 ± 0.03	1.6 ± 0.12
		Coarse	17 ± 0.62	126 ± 23	13 ± 4.2	0.34 ± 0.10	0.22 ± 0.08	0.11 ± 0.04	0.87 ± 0.02	1.1 ± 0.05	0.35 ± 0.01
Cropland on the slope	Upper	Fine	10 ± 0	33 ± 0.9	54 ± 1.5	1.3 ± 0.04	1.5 ± 0.14	1.7 ± 0.03	1.0 ± 0.01	0.77 ± 0.02	1.2 ± 0.02
		Coarse	20 ± 0.32	172 ± 16	7.8 ± 0.50	0.47 ± 0.03	0.26 ± 0.02	0.12 ± 0.01	0.74 ± 0.01	1.0 ± 0.05	0.54 ± 0.03
	Middle	Fine	10 ± 0	30 ± 1.5	50 ± 0.42	1.5 ± 0.02	1.5 ± 0.15	1.7 ± 0.04	1.0 ± 0.03	0.88 ± 0.03	1.3 ± 0.09
		Coarse	16 ± 0.51	119 ± 12	6.8 ± 0.64	0.36 ± 0.05	0.22 ± 0.03	0.11 ± 0.01	0.78 ± 0.03	0.89 ± 0.06	0.43 ± 0.05
	Lower	Fine	10 ± 0	28 ± 1.6	59 ± 0.74	1.5 ± 0.01	1.4 ± 0.06	1.8 ± 0.07	1.0 ± 0.01	0.93 ± 0.02	1.3 ± 0.04
		Coarse	18 ± 0.28	167 ± 19	6.0 ± 0.90	0.41 ± 0.02	0.22 ± 0.03	0.08 ± 0.01	0.75 ± 0.01	0.81 ± 0.04	0.42 ± 0.02
Flood plain	FPF	Fine	10 ± 0	54 ± 2.7	53 ± 3.7	1.5 ± 0.13	1.6 ± 0.09	1.6 ± 0.09	1.0 ± 0.03	0.92 ± 0.04	1.5 ± 0.09
		Coarse	18 ± 0.91	157 ± 27	6.5 ± 1.9	0.30 ± 0.07	0.17 ± 0.04	0.11 ± 0.02	0.78 ± 0.02	0.87 ± 0.05	0.26 ± 0.01
	FPP	Fine	11 ± 0.5	46 ± 3.5	65 ± 2.0	1.6 ± 0.12	1.6 ± 0.06	1.8 ± 0.04	1.2 ± 0.02	1.2 ± 0.03	1.8 ± 0.08
		Coarse	20 ± 0.53	241 ± 20	5.2 ± 0.60	0.31 ± 0.02	0.17 ± 0.02	0.07 ± 0.01	0.84 ± 0.01	0.87 ± 0.05	0.39 ± 0.03

Data are the mean of each depth in the A horizon ± SE

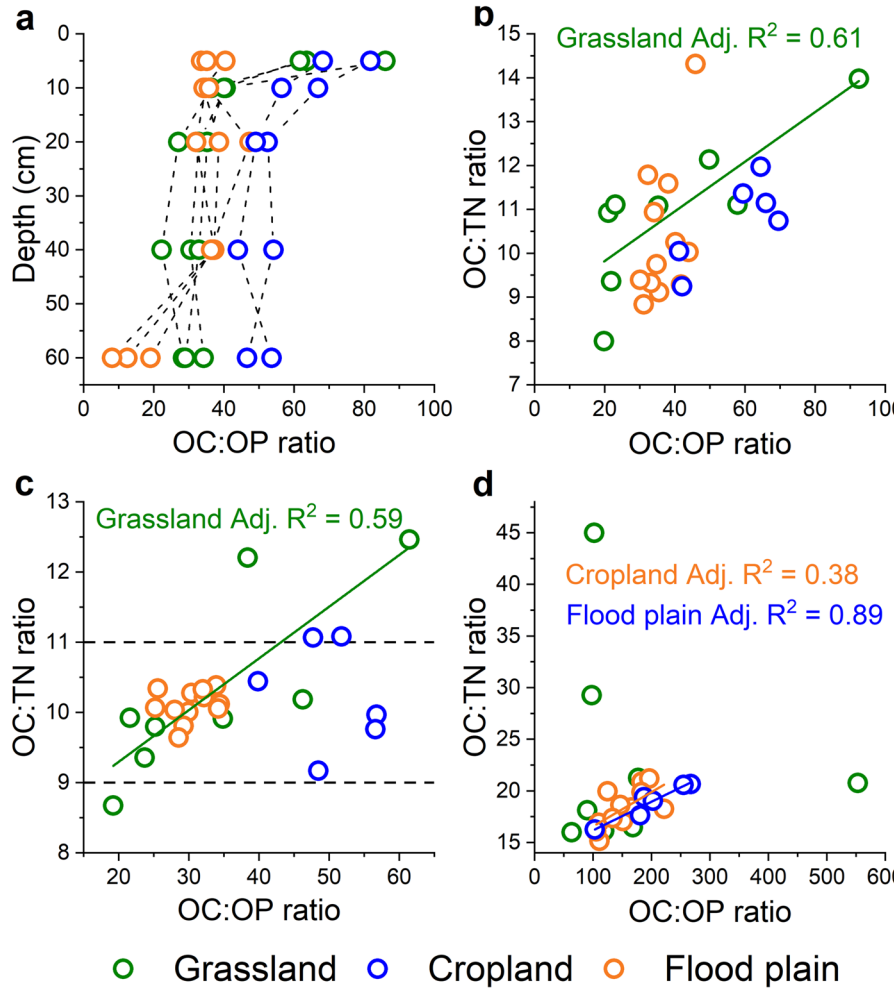

Fig. 4 **a** The OC:OP ratio down to 60 cm in bulk soil. Data are given as mean values of soil profile and three soil cores. **b** OC:TN ratio to OC:OP ratio in the bulk soil of A horizon in the soil profile, **c** OC:TN ratio to OC:OP ratio in the fine fraction of the A horizon in the soil profile, **d** OC:TN ratio to OC:OP ratio in the coarse fraction of A horizon in the soil profile. Detailed statistical results can be found in Table S.11

mineral-P depletion and soil degradation. Due to low SOM enrichment of subsoil (Table S.2), and high variation of OC and OP recovery during soil fractionation in the subsoil (data not presented), only the topsoil (A horizon) was further fractionated.

In the bulk soil, grasslands tend to have a higher OP/TP proportion than cropland due to more fresh SOM input. This is indicated by a lower alkyl:O-alkyl-C ratio (Table 1), and better SOM retention through decreased gaseous and hydrological N losses as derived from lower ^{15}N signature in the topsoil. However, no differences were measured between the hillslope and the flood plain (Fig. S.1). In the fine fraction (< 20 µm), predominantly consisting of MAOM fractions, OC, TN, and OP are primarily enriched, while IP dominates the coarse fraction (> 20 µm), containing mainly POM fractions (Just et al. 2021) (Fig. 3; Table 2), regardless of land use and soil development processes. Over 70% of OC and 85% of OP were found in the fine fraction, consistent with findings from soils in tropical, subtropical, and temperate zones (Spohn 2020b). An enrichment factor greater than 1 for both OC and OP in the fine fraction (Table 2) further supports this finding. Thus, long-term land use and soil development processes show limited effects on the overall allocation of OC and OP to the soil fractions of the A horizon.

However, the quantitative OP/TP proportions in the fine fraction reflect significant influence from the land use (Table 2), with grassland showing greater enrichment than the cropland, consistent with differences in mean OP content in the topsoil (Table S.3). This suggests that alterations in topsoil

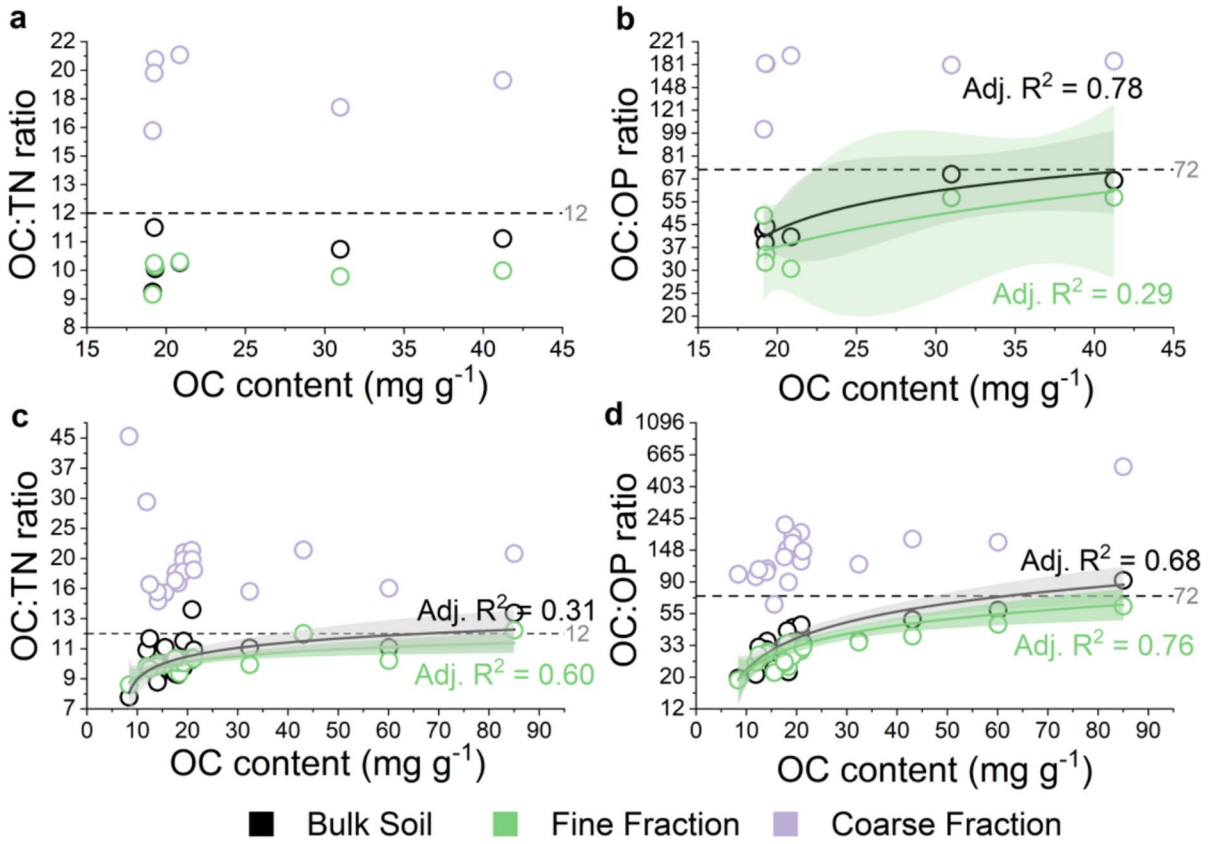

Fig. 5 **a** The OC:TN ratio to OC content and **b** the OC:OP ratio to OC content in the A horizon of soil profile in the flood plain. **c** The OC:TN ratio to OC content and **d** the OC:OP ratio to OC content in the A horizon of soil profile on the slope. To meet the normal distribution for regression, the OC:TN and OC:OP ratio was natural log transformed. The logarithmic regression was applied. The data presented are derived from the A horizon of the soil profiles. Detailed regression results are shown in Table S.11

OP content due to different land uses may primarily be driven by processes associated with OP allocation in the fine fraction. In addition, the OP compounds, particularly IHP, generally show greater resistance to solubiliztion than many IP compounds (except for primary-IP and those reprecipitated-secondary-P at specific pH) in the topsoil (Sulieman and Mühling 2021). This resilience is due to the stronger adsorption of OP to SOM (enhanced by multiple phosphate groups) and the higher stability of smaller particles, particularly clay-sized minerals, which can form aggregates that resist soil structural degradation (Nguyen et al. 2016; Berhe et al. 2018). The higher enrichment of OP in the fine fraction thus indicates a higher resistance to both soil structural degradation and solubilization, while the lower OP enrichment in the fine fraction of cropland soils may thus indicate weaker resistance.

These data highlight the distinct partitioning of OP and IP in different soil fractions under various land use and soil development processes. Grassland soils have a higher overall OP/TP proportion compared to the cropland soils, with OC, TN, and OP being primarily enriched in the fine fraction (< 20 µm), while IP is enriched in the coarse fraction (> 20 µm). Land use thus affects the OP content of the fine fractions, and the general stability of P contents during soil degradation.

The proximity of OC:OP ratio to microbial biomass C:P ratio indicates OP cycling pathways (biotic or abiotic) in the fine fraction

The distinct OC:TN ratio of microbial and plant-derived carbon sources (Angst et al. 2021; Kögel-Knabner 2002) supports the use of the OC:TN ratio as a qualitative indicator for OC storage potential (Cotrufo et al. 2019). An enrichment of OC in the MAOM fraction, coupled with a narrow OC:TN ratio, suggests that a significant proportion of OC, including some plant-derived sources (Kindler et al. 2009), has been decomposed and assimilated into microbial biomass/necromass. This OC is chemically bonded with minerals and physically protected in aggregates (Kögel-Knabner 2008), resulting in an N-rich MAOM fraction with an OC:TN ratio close to that of microbial biomass (Cotrufo et al. 2019). Considering a similar contribution and enrichment of OP as OC in soil fractions, Spohn (2020a, 2020b) suggests that OP follows a similar stabilization pathway as OC, with a substantial amount of OP cohesively stored with OC, which implies a significant OP assimilation within microbial biomass/necromass and subsequent association with mineral surfaces.

In our soils, the OC:TN ratio in the A horizon ranges from 9:1 to 11:1 in the fine fraction (Fig. 4c), indicating a high proportion of OC assimilated in microbial biomass/necromass (Cotrufo et al. 2019; Kögel-Knabner 2008). The similar distribution and enrichment patterns of OP and OC, along with a narrow OC:TN ratio and a narrow OC:OP ratio (ranging from 20:1 to 72:1) in the fine fraction, are consistent with findings from various soils worldwide (Kirkby et al. 2011). Therefore, this narrow OC:OP ratio, primarily within the range of microbial biomass C:P ratios (ranging from 23:1 to 100:1), may suggest OP assimilation within microbial biomass/necromass, correlating with N.

However, the OC and OP, as well as TN and OP show weaker correlations in the fine fraction compared to OC and TN (Table S.10), as also noted by Williams and Steinbergs (1958). Combined with the narrower OC:OP ratio relative to that of microbial biomass/necromass in the fine fraction, and a lower $\delta^{15}N$ signature (Fig. S.3) found in some A horizons of grassland soils on the hillslope, this may suggest an additional N-decoupled/N-depleted pathway for OP stabilization.

This abiotic pathway, independent of assimilation within N-rich microbial biomass, is indicated by a narrower OC:OP ratio than the microbial biomass C:P ratio in the fine fraction and a higher $\delta^{15}N$ signature. This represents a series of stable orthophosphate mono/diesters with C:P ratios ranging from 1:1 to 11:1, particularly inositol orthophosphate (generally absent of N). These compounds exhibit increased resistance to mineralization due to complex structural formation and chelation with the mineral phase (Condron et al. 2005; Huang et al. 2017), associating directly with mineral surfaces. This also aligns with the limited accumulation of carbohydrates found in those soils, as indicated by a higher alkyl:O-alkyl-C ratio (Table S.9).

The proximity of the OC:OP ratio in the fine soil fraction to the ratios of mono/diester orthophosphate groups (1:1–11:1), microbial biomass C:P (23:1–100:1), and plant materials (>>100:1 up to 6000:1) potentially indicates the composition and mineralization status of OP, as well as their dominant association pathways in the MAOM fraction. The grassland soils, with higher SOM compared to cropland soils, have a significant correlation between OC:TN and OC:OP ratios (Fig. 4), which may indicate the dominant of N-associated OP pathway in the MAOM fraction. Furthermore, both OC:TN and OC:OP ratios in the fine fraction increase linearly with higher OC content up to 85 mg OC g^{-1} in our study (Fig. 5; Table S.11), suggesting a greater proportion of less decomposed plant-derived C sources, resulting in higher OC:OP and OC:TN ratios in the fine fraction.

Based on this information, we suggest that the OC:OP ratio in the fine fraction can serve as an indicator of two different pathways (biotic and abiotic) of OP cycling in SOM and their dominance, influenced by environmental factors such as land use and soil development processes in our study. A narrower OC:OP ratio than the average microbial biomass C:P ratio in the fine fraction found in some A horizons of grassland soils on the hillslope may indicate a higher proportion of OP stabilized within the fine fraction via direct association with mineral surfaces. Conversely, a similar OC:OP ratio to the microbial biomass C:P ratio in the fine fraction suggests a greater proportion of OP stabilized through assimilation into microbial biomass/necromass. This interpretation is supported by the observed wider OC:OP ratio with

higher OC content (Fig. 5), indicative of the proportion and decomposition status of plant-derived C sources.

Conclusion

Our investigation of a temperate hillslope-flood plain system in South-East Germany reveals distinct impacts of long-term grassland and cropland use on OC, TN, and P stocks on the hillslope. Unique TP partitioning was observed under similar organic fertilization regimes, with croplands having higher IP stocks in the topsoil and lower OP stocks in the subsoil, whereas grassland exhibits the opposite pattern. The higher IP stocks in cropland topsoil counterbalance the lower OP stocks in the subsoil, resulting in comparable TP stocks between the two land uses. The grassland soils on the hillslope exhibit higher OC and TN stocks than cropland soils, attributed to greater topsoil SOM accumulation and well-preserved subsoils. Higher $\delta^{15}N$ isotopic signatures confirm lower N losses in grassland topsoil. In contrast, cropland experiences diminished OC and TN contents due to reduced SOM input and soil degradation.

The flood plain soils, developed from distinct processes by alluvial sediments and groundwater, are decoupled from the hillslope, leading to substantial contributions of OC, TN, and IP stocks from the subsoil. The long-term grassland use impacts SOM stocks confined to the topsoil.

Irrespective of land use and soil development processes, both OC and OP are enriched in the fine fraction (< 20 µm) and depleted in the coarse fraction (20–2000 µm). Further stoichiometric assessment showed a higher OP:TP ratio in the fine fraction of grassland than the cropland on the hillslope, which is consistent with a higher OP/TP proportion in the fine fraction. This indicates a higher resistance of grassland soils on the slope against soil degradation, due to stronger resistance of OP in the fine fraction derived from higher input and better retainment of SOM.

Similar to the OC:TN ratio as an indicator of OC stabilization potential, the OC:OP ratio in the fine fraction may indicate two pathways (biotic and abiotic) of OP cycling. A similar OC:OP ratio to the microbial biomass C:P ratio suggests a greater proportion of OP stabilized within microbial biomass/necromass, representing biotic pathway. The abiotic pathway, independent of assimilation within N-rich microbial biomass, is indicated by a narrower OC:OP ratio than the microbial biomass C:P ratio in the fine fraction. The OC:OP ratio can be impacted by both land use and soil development processes.

Our findings disentangle the distinct impact of land use and soil development processes on the stocks of OC, TN, and P. In particular, we show that an apparently similar stoichiometry of OC, TN and OP at the bulk soil level has limited explanatory power for the P partitioning (IP vs. OP) and stoichiometric correlations of OC:OP in soil fractions. Our results call for a closer investigation of OC, TN and OP stoichiometry and dynamics in different soil fractions. Reliable insights into OP storage and its biogeochemical cycling with other elements in SOM, soil microorganisms and reactive minerals surfaces can only be achieved by shifting the focus from studying overall OC, TN and OP stoichiometric ratios towards a detailed investigation of soil fractions and P partitioning.

Acknowledgements The authors gratefully acknowledge the support of Bayerisches Staatsministerium für Umwelt und Verbraucherschutz (StMUV) for granting this study [TKP-01KPB-78573]. Special thanks go to Peter Schad for soil classification. We also greatly appreciate the assistance of Bärbel Deischl, Sigrid Hiesch, Christine Pfab, and Gabriele Albert from the Chair of Soil Science, Technical University of Munich, in soil analysis. The fieldwork would not have been possible without the support of Jincheng Han from Karlsruhe Institute of Technology, Anna Holmer, Yuan Zhuang from the Chair of Geomorphology and Soil Science, Technical University of Munich, and Rubén Martínez-Cuesta from the Helmholtz Center Munich, as well as the students Anika Thurau, Ellen Beckers, Felix Oberhardt, Joline Birgmann, Maximilian Langer, Milena Strenge, Nick Schmitthenner and Nico Beck from University of Freiburg. We also acknowledge Andrea Seidl from the Chair of Geomorphology and Soil Science, Technical University of Munich, for her contributions to assisting soil texture analysis. We thank Ulrike Ostler from Karlsruhe Institute of Technology for stable isotope analyses, and Carolin Schlabs from Karlsruhe Institute of Technology for data evaluation. Additionally, we express our gratitude to Yahan Hu and Stephan Haug, from Technical University of Munich, for providing suggestions on data analysis. Lastly, we extend many thanks to Martin Wiesmeier and Jörg Prietzel for their invaluable feedback, which greatly improved the quality of this work.

Author contributions Conceptualization: Kaiyu Lei, Franziska B. Bucka, Jörg Völkel, Ingrid Kögel-Knabner; Methodology: Kaiyu Lei, Franziska B. Bucka, Christopher Just, Sebastian Floßmann, Ingrid Kögel-Knabner; Formal analysis and investigation: Kaiyu Lei; Writing—original draft

preparation: Kaiyu Lei, Michael Dannenmann, Jörg Völkel; Writing—review and editing: Kaiyu Lei, Franziska B. Bucka, Christopher Just, Sigrid van Grinsven, Michael Dannenmann, Jörg Völkel, Ingrid Kögel-Knabner; Funding acquisition: Jörg Völkel, Ingrid Kögel-Knabner; Supervision: Franziska B. Bucka, Ingrid Kögel-Knabner.

Funding Open Access funding enabled and organized by Projekt DEAL. This work was supported by the project 'Bayerische Landschaften im Klimawandel II [TKP01KPB-78573]' granted by Bayerisches Staatsministerium für Umwelt und Verbraucherschutz (StMUV).

Data availability The datasets generated during the current study are not publicly available, but can be available from the corresponding author on reasonable request.

Declarations

Conflict of interest All authors declare that they have no known competing financial interests or personal relationships that could have appeared to influence the work reported in this paper.

References

Agbenin JO, Tiessen H (1995) Phosphorus forms in particle-size fractions of a toposequence from northeast Brazil. Soil Sci Soc Am J 59:1687–1693. https://doi.org/10.2136/sssaj1995.03615995005900060026x

Ahlmann-Eltze C, Patil I (2021) ggsignif: R package for displaying significance brackets for 'ggplot2'. PsyArxiv. https://doi.org/10.31234/osf.io/7awm6

Alt F, Oelmann Y, Herold N, Schrumpf M, Wilcke W (2011) Phosphorus partitioning in grassland and forest soils of Germany as related to land-use type, management intensity, and land use–related pH. J Soil Sci Plant Nutr 174:195–209. https://doi.org/10.1002/jpln.201000142

Amadou I, Faucon MP, Houben D (2022) Role of soil minerals on organic phosphorus availability and phosphorus uptake by plants. Geoderma 428:116125. https://doi.org/10.1016/j.geoderma.2022.116125

Andreetta A, Chelli S, Bonifacio E, Canullo R, Cecchini G, Carnicelli S (2023) Environmental and pedological factors influencing organic carbon storage in Italian forest soils. Geoderma Reg 32:e00605. https://doi.org/10.1016/j.geodrs.2023.e00605

Angst G, Mueller KE, Nierop KG, Simpson MJ (2021) Plant-or microbial-derived? A review on the molecular composition of stabilized soil organic matter. Soil Biol Biochem 156:108189

Bates D, Maechler M, Jagan M (2023) Matrix: sparse and dense matrix classes and methods. https://CRAN.R-project.org/package=Matrix

Bayerisches Landesamt für Umwelt (2022) Digitale Geologische Karte 1:25000, Blatt 6840 Reichenbach, Augsburg. https://www.lfu.bayern.de/geologie/geo_karten_schriften/dgk25_uab/index.htm. Accessed 1 Dec 2023

Bayerisches Landesamt für Umwelt (2023) Statistik Hammermühle/Otterbach creek. Abflüsse (Jahresreihe 1957–2013). Bayerisches Landesamt für Umwelt (LfU), Augsburg. https://www.gkd.bayern.de/de/fluesse/abfluss/bayern/hammermuehle-15315000/statistik Accessed 1 Dec 2023

Berhe AA, Barnes RT, Six J, Marín-Spiotta E (2018) Role of soil erosion in biogeochemical cycling of essential elements: carbon, nitrogen, and phosphorus. Ann Rev Earth Planet Sci 46:521–548. https://doi.org/10.1146/annurev-earth-082517-010018

Borrelli P, Robinson DA, Fleischer LR et al (2017) An assessment of the global impact of 21st century land use change on soil erosion. Nat Commun 8:1–13. https://doi.org/10.1038/s41467-017-02142-7

Cade-Menun BJ, Bainard LD, LaForge K, Schellenberg M, Houston B, Hamel C (2017) Long-term agricultural land use affects chemical and physical properties of soils from southwest Saskatchewan. Can J Soil Sci 97:650–666. https://doi.org/10.1139/cjss-2016-0153

Catoni M, D'Amico ME, Zanini E, Bonifacio E (2016) Effect of pedogenic processes and formation factors on organic matter stabilization in alpine forest soils. Geoderma 263:151–160. https://doi.org/10.1016/j.geoderma.2015.09.005

Celi L, Barberis E (2005) Abiotic stabilization of organic phosphorus in the environment. Organ Phosphorus Environ. https://doi.org/10.1079/9780851998220.0113

Chaplot V, Poesen J (2012) Sediment, soil organic carbon and runoff delivery at various spatial scales. Slope 88:46–56. https://doi.org/10.1016/j.slope.2011.09.004

Christensen BT (1992) Physical fractionation of soil and organic matter in primary particle size and density separates. Adv Soil Sci 20:1–90. https://doi.org/10.1007/978-1-4612-2930-8_1

Cleveland CC, Liptzin D (2007) C: N: P stoichiometry in soil: is there a "Redfield ratio" for the microbial biomass? Biogeochemistry 85:235–252. https://doi.org/10.1007/s10533-007-9132-0

Condron LM, Turner BL, Cade-Menun BJ (2005) Chemistry and dynamics of soil organic phosphorus. In: Sims JT, Sharpley AN (eds) Phosphorus: agriculture and the

environment. American Society of Agronomy, Madison, pp 87–121. https://doi.org/10.2134/agronmonogr46.c4
Cordell D, White S (2011) Peak phosphorus: clarifying the key issues of a vigorous debate about long-term phosphorus security. Sustainability 3:2027–2049. https://doi.org/10.3390/su3102027
Cotrufo MF, Ranalli MG, Haddix ML, Six J, Lugato E (2019) Soil carbon storage informed by particulate and mineral-associated organic matter. Nat Geosci 12:989–994. https://doi.org/10.1038/s41561-019-0484-6
Douglas B, Martin M, Ben B, Steve W (2015) Fitting linear mixed-effects models using lme4. J Stat Softw 67:1–48. https://doi.org/10.18637/jss.v067.i01
Fanin N, Fromin N, Buatois B, Hättenschwiler S (2013) An experimental test of the hypothesis of non-homeostatic consumer stoichiometry in a plant litter–microbe system. Ecol Lett 16:764–772. https://doi.org/10.1111/ele.12108
Fox J, Weisberg S (2019) An R companion to applied regression, 3rd edn. Sage, Thousand Oaks
Gava CAT, Giongo V, Signor D, Fernandes-Júnior PI (2022) Land-use change alters the stocks of carbon, nitrogen, and phosphorus in a Haplic Cambisol in the Brazilian semi-arid region. Soil Use Manag 38:953–963. https://doi.org/10.1111/sum.12716
George TS, Giles CD, Menezes-Blackburn D et al (2018) Organic phosphorus in the terrestrial environment: a perspective on the state of the art and future priorities. Plant Soil 427:191–208. https://doi.org/10.1007/s11104-017-3391-x
Gerke J (2015) Phytate (inositol hexakisphosphate) in soil and phosphate acquisition from inositol phosphates by higher plants. A review. Plants 4:253–266. https://doi.org/10.3390/plants4020253
Gocke MI, Don A, Heidkamp A, Schneider F, Amelung W (2021) The phosphorus status of German cropland—an inventory of top and subsoils. J Soil Sci Plant Nutr 184:51–64. https://doi.org/10.1002/jpln.202000127
Griffiths BS, Spilles A, Bonkowski M (2012) C: N: P stoichiometry and nutrient limitation of the soil microbial biomass in a grazed grassland site under experimental P limitation or excess. Ecol Process 1:1–11. https://doi.org/10.1186/2192-1709-1-6
Guggenberger G, Christensen BT, Zech W (1994) Land-use effects on the composition of organic matter in particle-size separates of soil: I. Lignin and carbohydrate signature. Eur J Soil Sci 45:449–458. https://doi.org/10.1111/j.1365-2389.1994.tb00530.x
Hadley W (2016) ggplot2: elegant graphics for data analysis. Springer, New York
Harnois L (1988) The CIW index: a new chemical index of weathering. Sediment Geol 55:319–322. https://doi.org/10.1016/0037-0738(88)90137-6
Hedley M, Stewart J, Chauhan B (1982) Changes in inorganic and organic soil phosphorus fractions induced by cultivation practices and by laboratory incubations. Soil Sci Soc Am J 46:970–976. https://doi.org/10.2136/sssaj1982.03615995004600050017x
Heidari A, Osat M, Konyushkova M (2022) Geochemical indices as efficient tools for assessing the soil weathering status in relation to soil taxonomic classes. Slope 208:105716. https://doi.org/10.1016/j.slope.2021.105716
Heuck C, Weig A, Spohn M (2015) Soil microbial biomass C: N: P stoichiometry and microbial use of organic phosphorus. Soil Biol Biochem 85:119–129. https://doi.org/10.1016/j.soilbio.2015.02.029
Hobley EU, Murphy B, Simmons A (2018) Comment on "Soil organic stocks are systematically overestimated by misuse of the parameters bulk density and rock fragment content" by Poeplau et al. (2017). Soil 4:69–171. https://doi.org/10.5194/soil-4-169-2018
Huang LM, Jia XX, Zhang GL, Shao MA (2017) Soil organic phosphorus transformation during ecosystem development: a review. Plant Soil 417:17–42. https://doi.org/10.1007/s11104-017-3240-y
IUSS Working Group WRB (2015) World reference base for soil resources 2014. International soil classification system for naming soils and creating legends for soil maps. World Soil Resources Reports No. 106. FAO, Rome
Just C, Poeplau C, Don A, van Wesemael B, Kögel-Knabner I, Wiesmeier M (2021) A simple approach to isolate slow and fast cycling organic carbon fractions in central european soils—importance of dispersion method. Front Soil Sci 1:692583. https://doi.org/10.3389/fsoil.2021.692583
Kassambara A (2023) ggpubr: 'ggplot2' Based Publication Ready Plots. https://CRAN.R-project.org/package=ggpubr
Kautz T, Amelung W, Ewert F et al (2013) Nutrient acquisition from arable subsoils in temperate climates: a review. Soil Biol Biochem 57:1003–1022. https://doi.org/10.1016/j.soilbio.2012.09.014
Khan KS, Joergensen RG (2019) Stoichiometry of the soil microbial biomass in response to amendments with varying C/N/P/S ratios. Biol Fertil Soils 55:265–274. https://doi.org/10.1007/s00374-019-01346-x
Kindler R, Miltner A, Thullner M, Richnow HH, Kästner M (2009) Fate of bacterial biomass derived fatty acids in soil and their contribution to soil organic matter. Org Geochem 40:29–37. https://doi.org/10.1016/j.orggeochem.2008.09.005
Kirkby C, Kirkegaard J, Richardson A, Wade L, Blanchard C, Batten G (2011) Stable soil organic matter: a comparison of C:N:P:S ratios in Australian and other world soils. Geoderma 163:197–208. https://doi.org/10.1016/j.geoderma.2011.04.010
Kögel-Knabner I (2002) The macromolecular organic composition of plant and microbial residues as inputs to soil organic matter. Soil Biol Biochem 34:139–162. https://doi.org/10.1016/S0038-0717(01)00158-4
Kögel-Knabner I, Amelung W (2021) Soil organic matter in major pedogenic soil groups. Geoderma 384:114785. https://doi.org/10.1016/j.geoderma.2020.114785
Kögel-Knabner I, Guggenberger G, Kleber M, Kandeler E, Kalbitz K, Scheu S, Eusterhues K, Leinweber P (2008) Organo-mineral associations in temperate soils: Integrating biology, mineralogy, and organic matter chemistry. J Plant Nutr Soil Sci 171:61–82. https://doi.org/10.1002/jpln.200700048
Kopittke PM, Dalal RC, Finn D, Menzies NW (2017) Global changes in soil stocks of carbon, nitrogen, phosphorus, and sulphur as influenced by long-term agricultural

production. Glob Change Biol 23:2509–2519. https://doi.org/10.1111/gcb.13513
Kretzschmar R (1996) Kulturtechnisch-bodenkundliches Praktikum-Ausgewählte Labormethode-Eine Anleitung zum selbstständigen Arbeiten an Böden. Institut für Wasserwirtschaft und Landschaftsökologie der Universität Kiel, Kiel
Kuznetsova A, Brockhoff PB, Christensen RHB (2017) lmerTest Package: tests in linear mixed effects models. J Stat Softw 82:1–26. https://doi.org/10.18637/jss.v082.i13
Li Y, Sang J, Zou C, Zhang Q et al (2024) Impacts of conversion of cropland to grassland on the CNP stoichiometric dynamics of soil, microorganisms, and enzymes across China: a synthesis. CATENA 246:108456. https://doi.org/10.1016/j.catena.2024.108456
Liu M, Dannenmann M, Lin S et al (2015) Ground cover rice production systems increase soil carbon and nitrogen stocks at regional scale. Biogeosciences 12:4831–4840. https://doi.org/10.5194/bg-12-4831-2015
Martinez-Mena M, Almagro M, Garcia-Franco N, de Vente J, Garcia E, Fayos CB (2019) Fluvial sedimentary deposits as carbon sinks: organic carbon pools and stabilization mechanisms across a Mediterranean catchment. Biogeosciences 16:1035–1051. https://doi.org/10.5194/bg-16-1035-2019
Mayer S, Schwindt D, Steffens M, Völkel J, Kögel-Knabner I (2018) Drivers of organic carbon allocation in a temperate slope-floodplain slope under agricultural use. Geoderma 327:63–72. https://doi.org/10.1016/j.geoderma.2018.04.021
Mayer S, Kühnel A, Burmeister J, Kögel-Knabner I, Wiesmeier M (2019) Controlling factors of organic carbon stocks in agricultural topsoils and subsoils of Bavaria. Soil Tillage Res 192:22–32. https://doi.org/10.1016/j.still.2019.04.021
Mew M, Steiner G, Haneklaus N, Geissler B (2023) Phosphate price peaks and negotiations-Part 2: the 2008 peak and implications for the future. Resour Policy 83:103588. https://doi.org/10.1016/j.resourpol.2023.103588
Mueller CW, Koegel-Knabner I (2009) Soil organic carbon stocks, distribution, and composition affected by historic land use changes on adjacent sites. Biol Fertil Soils 45:347–359. https://doi.org/10.1007/s00374-008-0336-9
Nakagawa S, Schielzeth H (2013) A general and simple method for obtaining R2 from generalized linear mixed-effects models. Methods Ecol Evol 4:133–142. https://doi.org/10.1111/j.2041-210x.2012.00261.x
Nelson PN, Baldock JA (2005) Estimating the molecular composition of a diverse range of natural organic materials from solid-state ^{13}C NMR and elemental analyses. Biogeochemistry 72:1–34. https://doi.org/10.1007/s10533-004-0076-3
Neuwirth E (2022) RColorBrewer: ColorBrewer Palettes. https://CRAN.R-project.org/package=RColorBrewer
Nguyen VB, Nguyen QB, Zhang YW, Lim CYH, Khoo BC (2016) Effect of particle size on erosion characteristics. Wear 348:126–137. https://doi.org/10.1016/j.wear.2015.12.003
Paetsch L, Mueller CW, Rumpel C, Angst Š, Wiesheu AC, Girardin C, Ivleva NP, Niessner R, Kögel-Knabner I (2017) A multi-technique approach to assess the fate of biochar in soil and to quantify its effect on soil organic matter composition. Org Geochem 112:177–186. https://doi.org/10.1016/j.orggeochem.2017.06.012
Page A, Miller R, Keeney D (1982) Chemical and microbiolo bgical properties. Soil Science Society of America, Madison
Prout JM, Shepherd KD, McGrath SP, Kirk GJ, Haefele SM (2021) What is a good level of soil organic matter? An index based on organic carbon to clay ratio. Eur J Soil Sci 72:2493–2503. https://doi.org/10.1111/ejss.13012
Quinton J, Govers G, Van Oost K, Richard DB (2010) The impact of agricultural soil erosion on biogeochemical cycling. Nature Geosci 3:311–314. https://doi.org/10.1038/ngeo838
R Core Team (2023) R: a language and environment for statistical computing. R Foundation for Statistical Computing, Vienna. https://www.R-project.org/
Saunders W, Williams E (1955) Observations on the determination of total organic phosphorus in soils. J Soil Sci 6:254–267. https://doi.org/10.1111/j.1365-2389.1955.tb00849.x
Schmidt MW, Torn MS, Abiven S et al (2011) Persistence of soil organic matter as an ecosystem property. Nature 478:49–56. https://doi.org/10.1038/nature10386
Scholz RW, Wellmer FW, Mew M, Steiner G (2025) The dynamics of increasing mineral resources and improving resource efficiency: prospects for mid-and long-term security of phosphorus supply. Resour Conserv Recy 213:107993. https://doi.org/10.1016/j.resconrec.2024.107993
Spohn M (2020a) Increasing the organic carbon stocks in mineral soils sequesters large amounts of phosphorus. Glob Change Biol 26:4169–4177. https://doi.org/10.1111/gcb.15154
Spohn M (2020b) Phosphorus and carbon in soil particle size fractions: a synthesis. Biogeochemistry 147:225–242. https://doi.org/10.1007/s10533-019-00633-x
Stutter MI, Shand CA, George TS et al (2015) Land use and soil factors affecting accumulation of phosphorus species in temperate soils. Geoderma 257:29–39. https://doi.org/10.1016/j.geoderma.2015.03.020
Sulieman S, Mühling KH (2021) Utilization of soil organic phosphorus as a strategic approach for sustainable agriculture. J Plant Nutr Soil Sci 184:311–319. https://doi.org/10.1002/jpln.202100057
Sun H, Wu Y, Zhou J, Yu D, Chen Y (2022) Microorganisms drive stabilization and accumulation of organic phosphorus: an incubation experiment. Soil Biol Biochem 172:108750. https://doi.org/10.1016/j.soilbio.2022.108750
Szabó JA, Keller B, Centeri C, Hatvani IG, Kovács J, Szalai Z, Jakab G (2023) Varying particle size selectivity of soil erosion along a cultivated catena. Open Geosci 15:20220585. https://doi.org/10.1515/geo-2022-0585
Thomas JL, Jeffrey A, Vincent A, Jacob AL, Ben B (2021) margins: marginal effects for model objects. https://github.com/bbolker/margins
Tipping E, Somerville CJ, Luster J (2016) The C: N: P: S stoichiometry of soil organic matter.

Biogeochemistry 130:117–131. https://doi.org/10.1007/s10533-016-0247-z

Turner BL, Lambers H, Condron LM, Cramer MD, Leake JR, Richardson AE, Smith SE (2013) Soil microbial biomass and the fate of phosphorus during long-term ecosystem development. Plant Soil 367:225–234. https://doi.org/10.1007/s11104-012-1493-z

UCLA (2021) Linear Mixed Models. UCLA: Statistical Consulting Group. https://stats.oarc.ucla.edu/other/mult-pkg/introduction-to-linear-mixed-models/ Accessed 1 December 2023

Van Oost K, Quine T, Govers G, De Gryze S, Six J, Harden J, Ritchie J, McCarty G, Heckrath G, Kosmas C (2007) The impact of agricultural soil erosion on the global carbon cycle. Science 318:626–629. https://doi.org/10.1126/science.1145724

Völkel J (1995) Periglaziale Deckschichten und Böden im Bayerischen Wald und seinen Randgebieten als geogene Grundlagen landschaftsökologischer Forschung im Bereich naturnaher Waldstandorte. Borntraeger, Z. Geomorph. N.F. Suppl. 96, Berlin/Stuttgart

Von Sperber C, Stallforth R, Du Preez C, Amelung W (2017) Changes in soil phosphorus pools during prolonged arable cropping in semiarid grasslands. Eur J Soil Sci 68:462–471. https://doi.org/10.1111/ejss.12433

Walker T, Adams A (1958) Studies on soil organic matter: I. Influence of phosphorus content of parent materials on accumulations of carbon, nitrogen, sulfur, and organic phosphorus in grassland soils. Soil Sci 85:307–318

Weihrauch C, Weber CJ (2021) The enrichment of phosphorus in floodplain subsoils—a case study from the Antrift catchment (Hesse, Germany). Geoderma 385:114853. https://doi.org/10.1016/j.geoderma.2020.114853

Wickham H, Bryan J (2023) readxl: read excel files. https://CRAN.R-project.org/package=readxl

Wiesmeier M, Urbanski L, Hobley E, Lang B, von Lützow M, Marin-Spiotta E, van Wesemael B, Rabot E, Ließ M, Garcia-Franco N (2019) Soil organic carbon storage as a key function of soils—a review of drivers and indicators at various scales. Geoderma 333:149–162. https://doi.org/10.1016/j.geoderma.2018.07.026

Williams CJ, Steinbergs A (1958) Sulphur and phosphorus in some Eastern Australian soils. Aust J Agric Res 9: 483–491. https://doi.org/10.1071/AR9580483

Wu J, He ZL, Wei WX, O'donnell A, Syers J (2000) Quantifying microbial biomass phosphorus in acid soils. Biol Fertil Soils 32:500–507. https://doi.org/10.1007/s003740000284

Xu X, Thornton PE, Post WM (2013) A global analysis of soil microbial biomass carbon, nitrogen and phosphorus in terrestrial ecosystems. Glob Ecol Biogeogr 22:737–749. https://doi.org/10.1111/geb.12029